SECTION 4

PHYSICS OF RADIATION AND ION-PLASMA TECHNOLOGIES

UDC 669.296:621.793

STRUCTURE AND PROPERTIES OF COATINGS BASED ON FeCrAl AND Cr18Ni10T

V.A. Belous, M.A. Bortnitskaya, R.L. Vasilenko, V.N. Voyevodin, I.O. Klimenko, V.I. Kovalenko, I.V. Kolodiy, A.S. Kuprin, V.G. Marinin, V.D. Ovcharenko, M.A. Tikhonovsky
National Science Center "Kharkov Institute of Physics and Technology", Kharkiv, Ukraine
E-mail: Squirells06@gmail.com

The process of vacuum-arc deposition of protective coatings from multicomponent FeCrAl cathodes and 18Cr10NiT stainless steel onto fragments of Zr1Nb alloy claddings has been developed. The influence of the reaction atmosphere (vacuum, nitrogen, oxygen) during the deposition of coatings on their structure, mechanical and corrosion properties is investigated. Coatings deposited in vacuum from the Cr18Ni10T cathode have the best set of mechanical properties and corrosion resistance; whereas coatings based on FeCrAl require composition optimization. It has been established that coatings deposited from FeCrAl and stainless steel cathodes with a thickness of 20 μm significantly increase oxidation resistance and prevent the destruction of fuel cladding under exposure to air at 1150 °C for 1 h.

INTRODUCTION

Following a severe nuclear accident at Fukushima Station in Japan in 2011, the issue of fuel stability and reactor safety has attracted much attention in the world. As a result, the concept of accident tolerant fuel (ATF) has been developed with improved performance in normal operation, both in design and in design basis accidents [1]. Under normal reactor conditions fuel claddings are also subjected to various types of mechanical wear, which can lead to a violation of their integrity and leakage of radioactive products [2–4]. Various candidate materials have been investigated to replace or protect zirconium alloy fuel claddings, which are designed to reduce the oxidation rate of the traditional claddings at least 100 times at temperatures above 1000…1200 °C [1, 5]: SiC [6], Cr coatings [7, 8], FeCrAl alloys and coatings [9, 10], MAX-phases [11], and Mo claddings [10]. As a result of the conducted researches it is established that Cr coatings obtained by different methods of physical deposition, demonstrate the best protective properties in different test conditions [7, 10]. Compared to chromium FeCrAl alloys can be more resistant to vapor oxidation at higher temperatures [12, 13] due to the formation of protective Al_2O_3 film at the surface. In some studies it has been shown that the physical-mechanical properties of such coatings depend on the method of their formation [14–16].

The purpose of this work was to investigate the effect of the cathode composition (FeCrAl alloy brand X23Y5T and Cr18Ni10T stainless steel) and the reaction atmosphere on the structure and protective properties of coatings obtained by vacuum-arc deposition.

EXPERIMENTAL METHODS

The coating deposition experiments were performed on a vacuum-arc unit equipped with a plasma source with a magnetic cathode spot stabilization [17]. FeCrAl alloy and Cr18Ni10T stainless steel were used as cathodes. The cathode diameter is 60 mm. The arc discharge current in all experiments was 100 A. The coatings were deposited on polished stainless steel specimens Cr18Ni10T Ø 20 and 2 mm thickness and fragments of Zr1Nb alloy fuel tubes Ø 9.1 mm which rotated in the center of the chamber at a distance of 250 mm from the cathode. The initial vacuum was ~ 10^{-3} Pa, in which the surface of the samples was cleaned with metal plasma for 3 min at a negative voltage on the samples – 1300 V. The deposition of the coatings was carried out in a vacuum of ~ $2 \cdot 10^{-3}$ Pa (series 1 and 3) and under nitrogen pressure (series 2 and 4) or oxygen (series 5) ~ 0.05 Pa for 60 min. The negative bias potential of the samples was -50 V. The coating thickness was (20 ± 2) μm. The temperature of the samples during deposition did not exceed 450 °C.

The thickness of the coatings was measured using an MII-4 interference microscope using the "shadow knife method". The chemical composition was determined by energy dispersive X-ray spectroscopy – EDS (Oxford Link ISIS 300) at 20 kV. The surface morphology of the coatings was studied using a scanning electron microscope JSM 7001 F.

XRD analysis was performed on DRON-2.0 X-ray diffractometer in cobalt Co-Kα radiation using Fe selectively absorbing filter. Diffracted radiation was detected by a scintillation detector. Qualitative phase analysis was performed using the ICDD PDF-2 database. Estimating of substructural characteristics (crystallite size **D** and microstrains level **ε**) of the coatings is based on the broadening of diffraction peaks. The analysis was performed using Williamson-Hall method. The annealed silicon powder was taken as the standard sample to deconvolute physical and instrumental broadening.

The cavitation erosion of the samples was investigated at the stand described in [18]. The cavitation zone was formed below the end surface of the concentrator mounted in a water vessel at a distance of (0.5 ± 0.05) mm from the sample surface. Cavitation

erosion was determined by mass loss with an accuracy of ± 0.015 mg. Abrasive wear was measured using a plane-to-disk scheme by a weighted method over a fixed period of time. The disk made of material with rigidly fixed abrasive particles rotates with a linear speed of 4.38 m/s with a load on a flat sample of 2.2 N. The nature of the destruction of the surface of the samples was examined using an optical microscope MMR-4. Microhardness of the coatings was measured on a PMT-3 tester with a Vickers diamond indenter at a load of 1 N.

The average corrosion rate in a 3% aqueous NaCl solution was determined using the potentiostat PI50-1 in a standard electrochemical cell of NPP-2 at temperature of 20 °C. The anode polarization curves were obtained by changing the potential at a speed of 1 mV/s. The chloride-silver electrode was used as the reference electrode, and the results are relative to the normal hydrogen electrode.

Tests for oxidation resistance of the fuel tube fragments (Ø 9.1 mm, l = 10 mm) of Zr1Nb alloy with deposited coatings were performed by annealing in air at 1150 °C for one hour. After oxidation the samples were weighed on a laboratory balance VLR-20 with an accuracy of ± 0.015 mg.

RESULTS AND DISCUSSION

The results of the composition analysis of vacuum arc coatings obtained from FeCrAl and Cr18Ni10T cathodes are presented in Table 1.

Table 1

Concentrations of elements in cathodes and coatings from FeCrAl alloy and Cr18Ni10T

Cathode	Composition, wt.%						
	Fe	Cr	Al	Ni	O	N	other
FeCrAl	72.1	22.6	4.1	0.1	–	–	1.1
1 vacuum	66	34	0.2	–	0.1	0.2	0.1
2 nitrogen	63	23	3.6	–	0.1	7.6	2.7
Cr18Ni10T	69	18	–	10	–	–	3
3 vacuum	68.2	27.5	–	4	0.1	0.1	0.1
4 nitrogen	63.1	20.2	–	9.4	0.6	5.5	1.2
5 oxygen	71.3	17.2	–	9	2	0.1	0.4

The data in Table 1 and Fig. 1 show that the composition and morphology of coatings are largely dependent on the gas atmosphere during the deposition. In the coatings deposited in vacuum from the FeCrAl cathode virtually no aluminum; and in the coatings – from the cathode Cr18Ni10T significantly decreases the concentration of nickel with increasing Cr in both coatings compared to cathodes. The reason for this difference in the element concentration between the coatings and the cathodes may be the difference in their transport in the arc plasma and the selective sputtering of the sample surface [19].

The concentration of alloying elements in coatings obtained in nitrogen and oxygen is almost unchanged compared to the cathode composition, which can be explained by a decrease in the self-sputtering coefficient of the coating due to the decrease in the average charge of metal ions in the vacuum-arc plasma. It is known that for titanium plasma with increasing nitrogen pressure and/or distance from the cathode to the substrate, the charge and energy of the plasma particles change due to the scattering of ions on the gas target, which leads to a decrease in the average charge and ion energy [20].

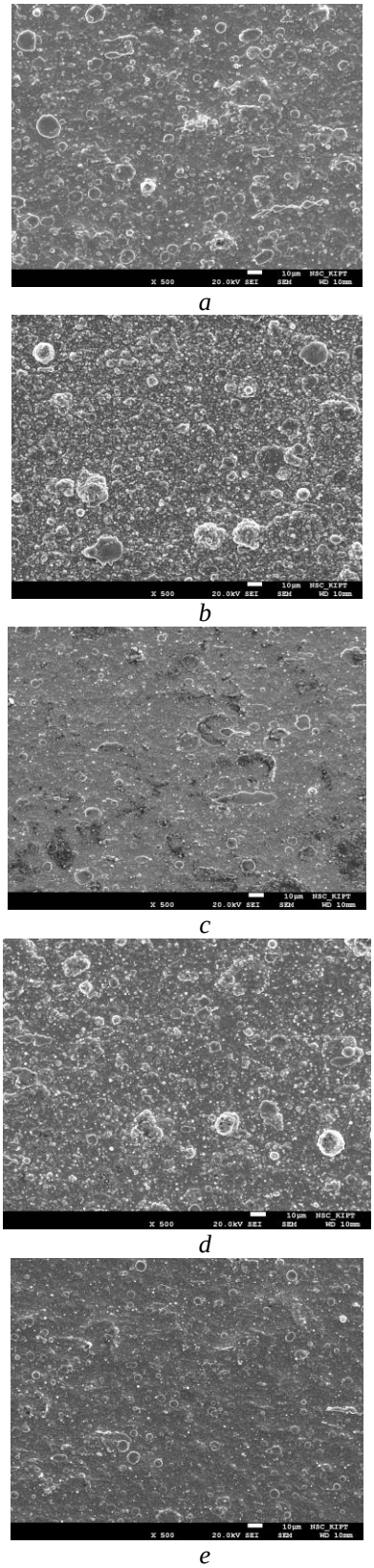

Fig. 1. Surfaces of coatings deposited from FeCrAl (a, b) and Cr18Ni10T (c, d, e) cathodes, in vacuum (a, c), under nitrogen (b, d) and oxygen (e) atmosphere

In the coatings deposited from the Cr18Ni10T cathode in an oxygen atmosphere (sample 5), the

concentration of nickel is the same as in the coating deposited in nitrogen one. The surface of the coatings is less developed and there are fewer macrodefects. This may be due to a change in the conditions of the cathode spot on the cathode surface.

Coatings deposited in vacuum from the FeCrAl and Cr18Ni10T cathodes have different surface morphologies and that they are almost identical in the nitrogen environment (see Fig. 1). There is a large number of macrodefects on the surface that can be identified as droplets of cathode material [19]. During the coatings depositing from different cathodes in nitrogen, the number and size of these defects are close, and in vacuum differ significantly.

The diffraction patterns of coatings deposited from the FeCrAl and the Cr18Ni10T cathodes in different atmospheres are shown in Fig. 2.

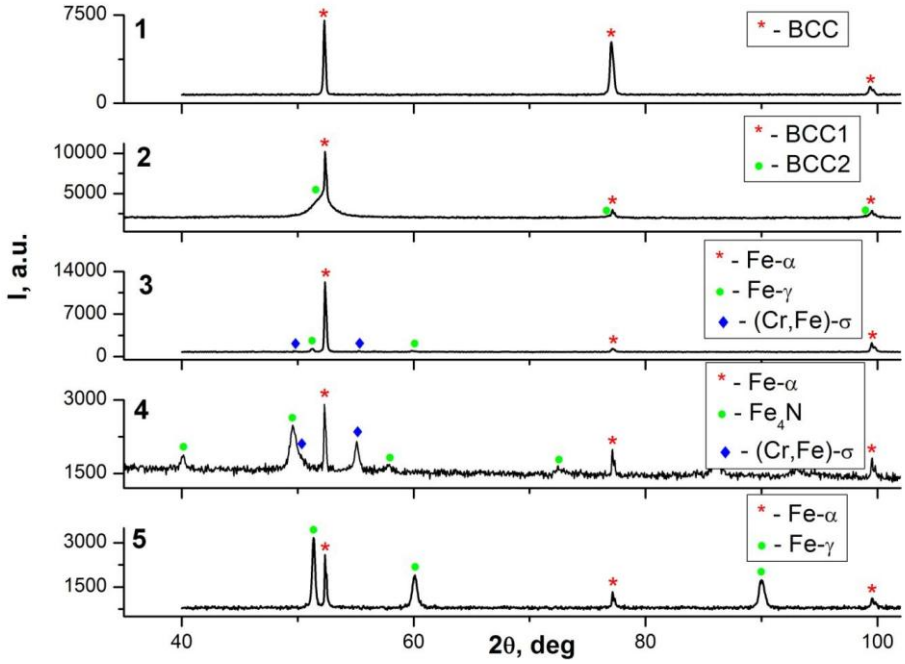

Fig. 2. The diffraction patterns of coatings deposited from the FeCrAl (1, 2) and the Cr18Ni10T cathodes (3–5): 1, 3 – in vacuum; 2, 4 – in nitrogen, and 5 – in oxygen

The data on the phase composition and structure of coatings are given in Table 2.

Table 2

Phase composition and structure of coatings

No.	Phase	Content, wt.%	Lattice parameters, Å	*D*, nm	ε, 10^{-3}
1	BCC	100	2.8758	227, 3	1.29
2	BCC1	15.3	2.8727	–	–
	BCC2	84.7	2.8871	10.3	7.48
3	Fe-α	90.6	2.8729	530.7	1.05
	Fe-γ	6.2	3.592	–	–
	(Cr, Fe)-σ	3.2	a = 8.81; c = 4.53	–	–
4	Fe-α	–	2.871	–	–
	Fe_4N	–	3.695	26.5	2.31
	(Cr, Fe)-σ	–	a = 8.82; c = 4.52	–	–
5	Fe-α	25.5	2.8718	–	–
	Fe-γ	74.5	3.5825	116.2	2.64

.

Data analysis in Table 2 confirms the significant influence of the atmosphere composition in which coatings are deposited.

In sample 1 (see Table 2), only the BCC phase with the lattice parameter a = 2.876 Å was detected. Relative intensity of the line (200) is higher than that for the powder distribution, which indicates the presence of texture (200) in the coating (part of the grains has a preferred orientation of crystallographic planes {200} parallel to the sample surface). The diffraction pattern also shows the lines broadening, so the calculation of substructural characteristics was performed. The crystallite size was D = 227.3 nm and the microstrain level was $\varepsilon = 1.29 \cdot 10^{-3}$.

The diffraction pattern of sample 2 (see Table 2) shows narrow diffraction lines that broadening considerably at the base. This is the effect of overlapping 2 types of lines that have close angular

positions but differ significantly in FWHM. I.e. there are 2 BCC phases in the sample with close lattice parameters, but significantly different in crystallite size: coarse-grained BCC1 (correspond to lines with small FWHM) and nanocrystalline BCC2 (correspond to lines with large FWHM). The weight content of the BCC1 phase in the sample is 15.3 wt.%, the lattice parameter is a = 2.873 Å. The crystallite size of this phase is large (microns – tens of microns). The weight content of the BCC2 phase in the sample is 84.7 wt.%, the lattice parameter is a = 2.887 Å. The lattice parameter of the BCC2 phase is larger than that for BCC1, that is probably due to the dissolution of the nitrogen in the BCC2 lattice. Estimated crystallite size of BCC2 phase was D = 10.3 nm and the microstrain level was $\varepsilon = 1.29 \cdot 10^{-3}$.

In sample 3 (see Table 2) revealed 3 phases: ferrite Fe-α, austenite Fe-γ and tetragonal phase (Cr, Fe)-σ. The main phase is ferrite Fe-α with the weight fraction in the sample of 90.6 wt.%, the lattice parameter is a = 2.873 Å. Crystallite size of the ferrite is D = 530.7 nm at the microstrain level of $\varepsilon = 1.05 \cdot 10^{-3}$. The content of austenite Fe-γ in the sample is 6.2 wt.%, lattice parameter is a = 3.592 Å. The content of σ-phase (Cr, Fe)-σ in the sample is 3.2 wt.%, the lattice parameters are: a = 8.81 Å; c = 4.53 Å. The calculation of the substructural characteristics for the austenite Fe-γ and σ-phase is difficult because of the low intensity of the lines. It should also be noted that the intensity distribution of the diffraction lines of all phases in the sample corresponds to the non-textured state.

In sample 4 (see Table 2) revealed 3 phases: Fe-α ferrite, iron nitride Fe_4N (cubic system, s.g. #222) and phase (Cr, Fe)-σ. It is difficult to determine the weight fraction of the phases in this sample. Lattice parameter of the ferrite is a = 2.871 Å. A weak texture (200) was detected in this phase. FWHM of the ferrite lines is comparable to the FWHM for standard sample, indicating a large crystallite size (microns – tens of microns). The lattice parameter of the nitride Fe_4N is a = 3.695 Å, D = 26.5 nm at the microstrain level $\varepsilon = 2.31 \cdot 10^{-3}$. The lattice parameters of the σ-phase are: a = 8.82 Å; c = 4.52 Å, crystallite size and microstrains were not determined.

In sample 5 (see Table 2) revealed 2 phases: Fe-α ferrite and austenite Fe-γ. The main phase is austenite Fe-γ, the weight fraction in the sample is 74.5 wt.%, the lattice parameter is a = 3.583 Å. The intensity distribution of austenite diffraction lines indicates the presence of a weak texture (220). The calculation of the substructural characteristics showed that the crystallite size of austenite is D = 116.2 nm at microstrain level of $\varepsilon = 2.64 \cdot 10^{-3}$. The content of Fe-α ferrite in the sample is 25.5 wt.%, the lattice parameter is a = 2.872 Å. Weak texture (200) was detected in the ferrite. FWHM of the ferrite lines is comparable to FWHM of the lines of the standard sample, indicating a large crystallite size (microns – tens of microns).

The influence of the atmosphere in which coatings are deposited from different cathodes on the rate of destruction by the action of abrasive and cavitation-induced micro-shocks is shown in Figs. 3, 4.

Fig. 3 shows the kinetic curves of the mass loss of the coatings on the time of cavitation.

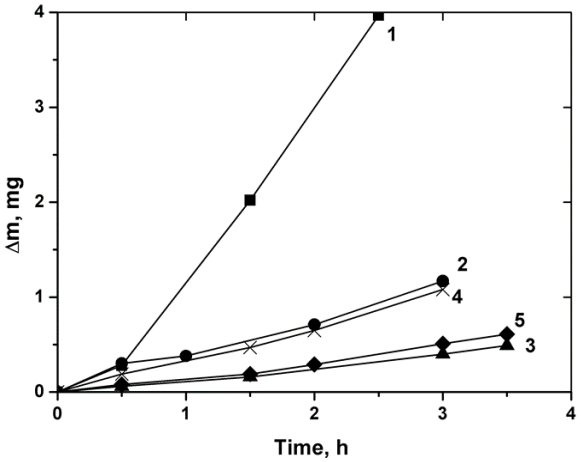

Fig. 3. Kinetic curves of coatings mass loss (Δm) from the time of cavitation: FeCrAl (1, 2) and Cr18Ni10T (3–5) cathodes: 1, 3 – vacuum; 2, 4 – in the nitrogen, and 5 – oxygen atmosphere

From the Fig. 3 data shows that the rate of destruction of coatings obtained in vacuum, the smallest when deposited from the cathode Cr18Ni10T (curve 3), and the largest – from the FeCrAl cathode in vacuum (curve 1). Coating (2, 4) deposited from different cathodes in the nitrogen atmosphere have smaller and similar values of the rate of mass loss during the cavitation action. The coating obtained from the Cr18Ni10T cathode in the oxygen atmosphere is also resistant to microshock destruction.

The results of measuring the wear of the coatings under the action of abrasive are shown in Fig. 4.

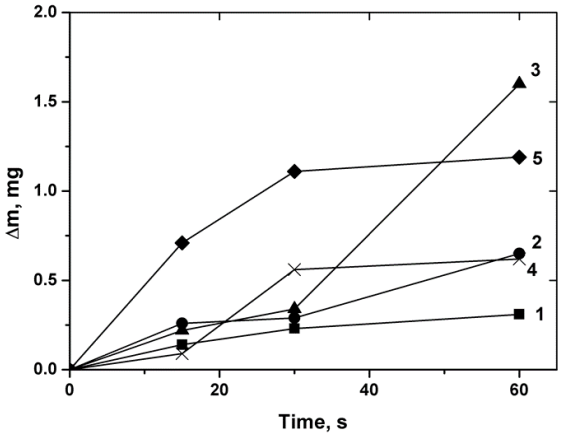

Fig. 4. Weight loss (Δm) of coatings, depending on the time of abrasive action: FeCrAl (1, 2) and Cr18Ni10T (3–5) cathodes: 1, 3 – in vacuum, 2, 4 – in the nitrogen, and 5 – oxygen atmosphere

The best abrasion resistance under friction shows the coating deposited from FeCrAl cathode in vacuum. Data analysis Fig. 4 shows that, as with the action of cavitation, the mass loss during abrasive wear of coatings deposited in nitrogen atmosphere from different cathodes is close (curves 2, 4). Their microhardness (H_μ) is also close (12.7 and 12.1 GPa, respectively). Coatings deposited in oxygen atmosphere from the Cr18Ni10T cathode have values of H_μ and the

fracture rates are 1.2 times lower in comparison with the coatings in vacuum.

The average mass fracture rates determined by kinetic curves (see Fig. 3) are listed in the value of the rate of increase in the depth of fracture of coatings. In addition, microhardness and fracture rate measurements during abrasive exposure were made. The results are presented in Table 3.

Table 3

Mechanical characteristics of coatings
(H_μ – Vikers microhardness of coatings; v_k – constant rate of destruction under the influence of cavitation; v_a – rate of destruction during abrasive wear)

Parameter	Number of the samples				
	1	2	3	4	5
H_μ, GPa	2.38	12.7	3.48	12.1	2.82
$v_{k,}$ μm/h	7.28	2.1	0.64	1.89	0.81
$v_{a,}$ mg/h	18.6	39.3	97	39.3	72

The data in Table 3 show that the coatings deposited in vacuum using Cr18Ni10T cathode have H_μ value 1.46 times large than in coatings from FeCrAl alloy, v_a a 5.2 times more, and v_k 11.4 times smaller. Coatings deposited in nitrogen atmosphere from these cathodes have close values of H_μ, v_a, and v_k. The coatings (5) deposited in the oxygen atmosphere have values of H_μ, v_a in 1.23 and 1.35 times smaller than the coatings obtained in vacuum, and – v_k 1.26 times more.

In order to determine the influence of the parameters of the deposition process on the corrosion resistance of coatings, their study was performed by potentiometry. The polarization curves of the coatings in 3% NaCl solution are shown in Fig. 5.

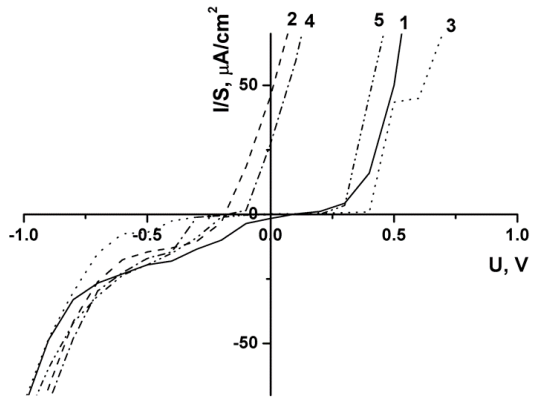

Fig. 5. Polarization curves of coatings in 3% NaCl solution deposited from FeCrAl (1, 2) and Cr18Ni10T (3–5) cathodes: (1, 3) – in vacuum; (2, 4) – in the nitrogen, and 5 in oxygen atmosphere

Analysis of the polarization curves (see Fig. 5) shows that the potential of the beginning of corrosion dissolution (φ_{nk}) takes values: +0.075; -0.195; +0.08; -0.185; +0.07 V for coatings 1–5, respectively. It can be seen that the values of φ_{nk} for coatings 2 and 4 are close and negative, and for 1, 3, and 5 are shifted to a more positive region, which indicates their sufficiently high corrosion resistance. Thus, coatings obtained from 2 different composition cathodes, but at the same nitrogen pressure have not only close values of mechanical but also corrosion properties.

In order to determine the effect of the parameters of the deposition process of the coatings on the oxidation resistance of the fuel claddings fragments, their annealing was carried out in an air atmosphere at a temperature of T = 1150 °C for one hour (Table 4).

Table 4

Photographs of Zr1Nb zirconium alloy tube fragments after annealing in air at 1150 °C for one hour: (0 – uncoated), with coatings deposited from FeCrAl cathode (1, 2) and Cr18Ni10T cathode (3–5); (1, 3) in vacuum; (2, 4) in nitrogen, and (5) in oxygen

Sample No.	0	1	2	3	4	5
Before Oxidation						
After Oxidation						

The photos in Table 4 show how the color of the surface changes from metallic to white with brown spots after oxidation, due to the formation of the oxide layer in the uncoated tube. At the same time, the coated tubes deform much less and have green or black color of the oxide layer. This color of the surface of the protective coatings after oxidation may indicate the formation of chromium oxides in the surface layer.

Mass gain of the coated tubes (3…5 mg/cm^2) is an order of magnitude smaller than that of the uncoated tube (40 mg/cm^2), indicating a high resistance to oxidation of all deposited coatings. The smaller mass gain of the protected tubes is also due to the much smaller deformation, which prevents catastrophic oxidation of not only the outer but also the inner surface of the tubes. From the above data on high-temperature oxidation, it is difficult to make a clear conclusion about the benefits of any of the coatings because the mass gains are very close, but these data clearly indicate that the developed coatings based on iron with a content of Cr at least 18 at% protect the Zr1Nb alloy from oxidation in air at T = 1150 °C for 1 h.

Thus, the results of the conducted researches testify to the prospect of studying the processes of synthesis and application of protective coatings on the basis of doped iron alloys.

CONCLUSIONS

Within vacuum-arc deposition from multicomponent cathodes (FeCrAl, Cr18Ni10T) in vacuum, aluminum and nickel concentration decreases in coatings regarding their content in cathodes.

XRD analysis of coatings obtained from the FeCrAl cathode in vacuum revealed the presence of single BCC phase; and two BCC phases in the nitrogen atmosphere: coarse-grained and nanocrystalline. The coatings from the Cr18Ni10T cathode have three phases in vacuum and nitrogen: (Fe-α ferrite, Fe-γ austenite and (Cr, Fe)-σ) and (Fe-α, Fe4N, (Cr, Fe)-σ) respectively, and there are two phases (Fe-α ferrite and Fe-γ austenite) in the oxygen atmosphere.

Coatings from a FeCrAl cathode in the nitrogen atmosphere have a resistance to destruction 3.5 times greater than those applied in vacuum under cavitation-induced micro-shock conditions. Obtained values can be increased by optimizing the coating deposition process. Coatings deposited in vacuum from the Cr18Ni10T cathode have the best set of mechanical properties.

All obtained coatings significantly increase the resistance to air oxidation of Zr1Nb alloy samples at 1150 °C for 60 min.

The corrosion resistance in 3% NaCl solution of coatings deposited in vacuum and oxygen is higher than in nitrogen atmosphere.

REFERENCES

1. S.J. Zinkle, K.A. Terrani, J.C. Gehin, L.J. Ott, L.L. Snead. Accident tolerant fuels for LWRs: a perspective // *J. Nucl. Mater.* 2014, v. 448(1), p. 374-379.

2. Hyung-Kyu Kim, Young-Ho Lee, Sung-Pil Heo. Mechanical and experimental investigation on nuclear fuel fretting // *Tribology International*. 2006, v. 39, p. 1305-1319.

3. Young-Ho Lee, Thak Sang Byun. A comparative study on the wear behaviors of cladding candidates for accident-tolerant fuel // *Journal of Nuclear Materials* 2015, v. 465, p.857-865.

4. K. Edsinger. EPRI and the zero fuel failures program // *The Nuclear News*. 2010, p. 40.

5. B.A. Pint, K.A. Terrani, Y. Yamamoto, L.L. Snead. Material selection for accident tolerant fuel cladding // *Metall. Mater. Trans. E.* 2015, v. 2(3), p. 190-196.

6. J.-Y. Park, I.-H. Kim, Y.-I. Jung, H.-G. Kim, D.-J. Park, W.-J. Kim. Long-term corrosion behavior of CVD SiC in 360 °C water and 400 °C steam // *J. Nucl. Mater.* 2013, v. 443(1), p. 603-607.

7. J.-H. Park, H.-G. Kim, J.-Y. Park, Y.-I. Jung, D.-J. Park, Y.-H. Koo. High temperature steam-oxidation behavior of arc ion plated Cr coatings for accident tolerant fuel claddings // *Surf. Coat. Technol.* 2015, v. 80, p. 256-259.

8. A.S. Kuprin, V.A. Belous, V.V. Bryk, R.L. Vasilenko, V.N. Voyevodin, V.D. Ovcharenko, G.N. Tolmachova, I.V. Kolodiy, V.M. Lunyov, I.O. Klimenko. Vacuum-arc chromium coatings for Zr-1Nb alloy protection against high-temperature oxidation in air // *Problems of Atomic Science and Technology*. 2015, N 2(96), p. 111-118.

9. D.J. Park, H.G. Kim, J.Y. Park, Y.I. Jung, J.H. Park, Y.H. Koo. A study of the oxidation of FeCrAl alloy in pressurized water and high-temperature steam environment // *Corros. Sci.* 2015, v. 94, p. 459-465.

10. K.A. Terrani. Accident tolerant fuel cladding development: Promise, status, and challenges // *Journal of Nuclear Materials*. 2018, v. 501, p. 13-30.

11. Z. Duan, H. Yang, Y. Satoh, K. Murakami, S. Kano, Z. Zhao, J. Shen, H. Abe. Current status of materials development of nuclear fuel cladding tubes for light water reactors // *Nuclear Engineering and Design*. 2017, v. 316, p. 131-150.

12. K.A. Terrani, S.J. Zinkle, L.L. Snead. Advanced oxidation-resistant iron-based alloys for LWR fuel cladding // *Journal of Nuclear Materials.* 2014, v. 448, p. 420-435.

13. K.A. Terrani, C.M. Parish, D. Shin, B.A. Pint. Protection of zirconium by alumina-and chromia-forming iron alloys under high-temperature steam exposure // *J. Nucl. Mater.* 2013, v. 438(1), p. 64-71.

14. X. Han, Y. Wang, S. Peng, H. Zhang. Oxidation behavior of FeCrAl coated Zry-4 under high temperature steam environment // *Corrosion Science*. 2019, v. 149, p. 45-53.

15. J.G. Gigax, M. Kennas, H. Kim, B.R. Maier, H. Yeom, G.O. Johnson, K. Sridharan, L. Shao. Interface reactions and mechanical properties of FeCrAl-coated Zircaloy-4 // *Journal of Nuclear Materials*. 2019, v. 519, p. 57-63.

16. D. Park, P.A. Mouche, W. Zhong, K.K. Mandapaka, G.S. Was, B.J. Heuser. TEM/STEM study of Zircaloy-2 with protective FeAl(Cr) layers under simulated BWR environment and high-temperature steam exposure // *J. Nucl. Mater.* 2018, v. 2, p. 95-105.

17. V.M. Khoroshikh, S.A. Leonov, V.A. Belous. Features of the process of vacuum-arc produced Ti-plasma flux deposition under gas pressure of 1 to 10 Pa // *Surface and Coatings Technology*. 2015, v. 261, p. 167-173.

18. V.G. Marinin, V.I. Kovalenko, N.S. Lomino, Yu.A. Zadneprovsky, V.D. Ovcharenko. Cavitation erosion of Ti coatings produced by the vacuum arc method // *International Symposium on Discharges and Electrical Insulation in Vacuum, ISDEIV*. 2000, v. 2, p. 567-570.

19. I.I. Aksenov, V.A. Belous, Yu.A. Zadneprovskiy, A.S. Kuprin, N.S. Lomino, V.D. Ovcharenko, O.V. Sobol. Influence of nitrogen pressure on silicon content in Ti-Si-N coatings deposited by the vacuum-arc method // *Proceedings – International Symposium on Discharges and Electrical Insulation in Vacuum, ISDEIV*. 2010, art. no. 5625887, p. 497-500.

20. I.I. Aksenov, V.M. Khoroshikh. The influence of nitrogen on the erosion plasma ion component in a vacuum-arc source // *International Symposium on Discharges and Electrical Insulation in Vacuum, ISDEIV*. 1998, v. 2, p. 573-576.

Article received 10.02.2020

СТРУКТУРА И СВОЙСТВА ПОКРЫТИЙ НА ОСНОВЕ FeCrAl И Х18Н10Т

В.А. Белоус, М.А. Бортницкая, Р.Л. Василенко, В.Н. Воеводин, И.О. Клименко, В.И. Коваленко, И.В. Колодий, А.С. Куприн, В.Г. Маринин, В.Д. Овчаренко, М.А. Тихоновский

Разработан процесс вакуумно-дугового нанесения защитных покрытий из многокомпонентных катодов FeCrAl и нержавеющей стали Х18Н10Т на фрагменты твэльных оболочек из сплава Zr1Nb. Исследовано влияние реакционной атмосферы (вакуума, азота, кислорода) при осаждении покрытий на их структуру, механические и коррозионные свойства. Лучшим комплексом механических свойств и коррозионной стойкостью обладают покрытия, осажденные в вакууме из катода Х18Н10Т, а покрытия на основе FeCrAl требуют оптимизации состава. Установлено, что покрытия, осажденные из катодов типа фехраль и нержавеющей стали толщиной 20 мкм, существенно повышают устойчивость к окислению и предотвращают разрушение оболочек твэлов в условиях выдержки в воздухе при температуре 1150 °С в течение 1 ч.

СТРУКТУРА І ВЛАСТИВОСТІ ПОКРИТТІВ НА ОСНОВІ FeCrAl і Х18Н10Т

В.А. Білоус, М.О. Бортницька, Р.Л. Василенко, В.М. Воєводін, І.О. Клименко, В.І. Коваленко, І.В. Колодій, О.С. Купрін, В.Г. Марінін, В.Д. Овчаренко, М.А. Тихоновський

Розроблено процес вакуумно-дугового нанесення захисних покриттів з багатокомпонентних катодів FeCrAl і нержавіючої сталі Х18Н10Т на фрагменти твельних оболонок зі сплаву Zr1Nb. Досліджено вплив реакційної атмосфери (вакууму, азоту, кисню) під час осадження покриттів на їх структуру, механічні та корозійні властивості. Найкращим комплексом механічних властивостей та корозійною стійкістю володіють покриття, осаджені у вакуумі з катоду Х18Н10Т, а покриття на основі FeCrAl вимагають оптимізації складу. Встановлено, що захисні покриття, осаджені з катодів типу фехраль та нержавіючої сталі товщиною 20 мкм, суттєво підвищують стійкість до окислення та запобігають руйнуванню оболонок твелів в умовах витримки в повітрі при температурі 1150 °С впродовж 1 год.